PS Controls on the Distribution and Geometries of Sandstone Bodies in Platform Carbonate Systems: Examples from the Middle Permian (Guadalupian), Permian Basin, Texas*

Stephen C. Ruppel[1] and Robert G. Loucks[1]

Search and Discovery Article #50451 (2011)
Posted July 31, 2011

*Adapted from poster presentation at AAPG Annual Convention and Exhibition, Houston, Texas, USA, April 10-13, 2011

[1]Bureau of Economic Geology, University of Texas, Austin, TX (stephen.ruppel@beg.utexas.edu) .

Abstract

Although mixed shallow-water platform systems containing both carbonate and siliciclastic facies are common in the geological record, the processes that lead to this admixture and the geometries of the resulting facies are not well understood. Detailed, core-based study of two producing oil fields in the Permian Basin (Permian Grayburg Formation) has shed important light on these questions.

We examined more than 16,000 ft of core from 54 wells in two fields along the eastern side of the Central Basin Platform. Cores were used to define facies, stacking patterns and cyclicity and pore types. Core data were also used to calibrate wireline logs as a basis for defining field-wide correlations and sequence architecture.

Both fields display similar assemblages of carbonate and siliciclastic facies and record a similar accommodation history. By contrast, the abundance, distribution, and reservoir quality of siliciclastic facies (sandstone, siltstone, and siliciclastic-rich carbonate) in the two reservoirs vary widely. In South Cowden reservoir, siliciclastics are limited to a few intervals associated with cycle-scale flooding surfaces and transgressions and are non-porous. In North Cowden field, 20 mi (32 km) to the north, siliciclastics are locally thicker, are found in both transgressive (TST) and highstand (HST) systems tracts, and contain significant porosity and permeability.

Essentially all of these siliciclastics can be tied to low-accommodation sedimentation associated with early TST or late HST. This association is consistent with enhanced flux of siliciclastics onto carbonate platforms during sealevel fall and lowstand and is supported by both outcrop and subsurface studies of other Permian successions.

Data from North Cowden field suggest two distinctly different patterns of siliciclastic bed geometries. Siliciclastics associated with major flooding events (e.g., composite or third-order sequences) display greater continuity (along both strike and dip), although they are commonly thinner and of lower reservoir quality. Siliciclastics associated with high-frequency sequence (HFS) flooding events, by contrast, display

limited dip continuity but are thicker and of higher reservoir quality. In many cases they are developed as thick strike-elongate successions immediately distal to backstepping tidal-flat complexes. These geometries may be the result of more pronounced topographic relief produced by high rates of aggradation during HFS sedimentation.

Selected Bibliography

Jennings, J.W., Jr., F.J. Lucia, and S.C. Ruppel, 1998, Waterflood performance modeling for the South Cowden Grayburg reservoir, Ector County, Texas: The University of Texas at Austin, Bureau of Economic Geology Report of Investigations No. 247, 46 p.

Kerans, C., 1996, What's new in carbonates for 1996: Geotimes, v. 42/ 2, p. 51–52.

Kerans, C., and S.C. Ruppel, 1994, San Andres sequence framework, Guadalupe Mountains: implications for San Andres type section and subsurface reservoirs, *in* R.A. Garber, and D.R. Keller, (eds) Field guide to the Paleozoic section of the San Andres Mountains: Permian Basin Section: SEPM Publication No. 94-35, p. 105–115.

Lucia, F. J., 2000, Petrophysical characterization and distribution of remaining mobile oil: South Cowden Grayburg reservoir, Ector County, Texas: The University of Texas at Austin, Bureau of Economic Geology Report of Investigations No. 260, 54 p.

Lucia, F. J., and Ruppel, S. C., 1996, Characterization of diagenetically altered carbonate reservoirs, South Cowden Grayburg reservoir, West Texas: Society of Petroleum Engineers, Paper SPE 36650, p. 883–893.

Ruppel, S.C., Y.J. Park, and F.J. Lucia, 2002, Applications of 3-D seismic to exploration and development of carbonate reservoirs: South Cowden Grayburg field, West Texas, in Hunt, T. J., and Lufholm, P. H., eds., The Permian Basin: preserving our past—securing our future: West Texas Geological Society, Publication No. 02-111, p. 71–87.

Ruppel, S.C., and D.G. Bebout, 2001, Competing effects of depositional architecture and diagenesis on carbonate reservoir development: Grayburg Formation, South Cowden field, West Texas: The University of Texas at Austin, Bureau of Economic Geology Report of Investigations No. 263, 62 p.

Ruppel, S.C., and F.J. Lucia, 1996, South Cowden Grayburg field, Ector County, Texas, in Oil and gas fields in West Texas, v. VII: West Texas Geological Society, Publication No. 96-99, p. 39–48.

Ruppel, S.C., C. Kerans, R.P. Major, and M.H. Holtz, 1994, Controls on reservoir heterogeneity in Permian shallow-water platform carbonate reservoirs, USA: Implications for secondary recovery: The Arabian Journal for Science and Engineering, v. 19/2B, p. 215–236.

Controls on the Distribution and Geometries of Sandstone Bodies in Platform Carbonate Systems: Examples from the Middle Permian (Guadalupian), Permian Basin, Texas

Bureau of Economic Geology

Stephen C. Ruppel and Robert G. Loucks

Bureau of Economic Geology
Jackson School of Geosciences
The University of Texas at Austin
Austin, TX 78713-8924

Summary

Mixed shallow-water platform systems containing both carbonate and siliciclastic facies are common in the geological record. However, the processes that lead to this admixture, the geometries of these rocks, and their relative relationships to sealevel rise/fall events are not well understood. Detailed, core-based study of two producing oil fields in the Permian Basin (Permian Grayburg Fm) has shed important light on these questions.

We examined more than 16,000 ft of core from 54 wells in two fields along the eastern side of the Central Basin Platform. Cores were used to define facies, stacking patterns and cyclicity, and pore types. Core data were also used to calibrate wireline logs as a basis for defining field-wide correlations and sequence architecture.

Although both fields contain siliciclastics, their abundance, geometry, facies, and reservoir quality vary both within and between the two areas. At South Cowden field, siliciclastics are limited and non-porous. At North Cowden field, 20 mi (32 km) to the north, siliciclastics are more abundant, locally thicker, and contain significant porosity and permeability.

Data indicate two distinctly different styles of siliciclastic deposition, each associated with distinct geometries, sedimentary features, and reservoir properties. Both reflect LST sediment flux and TST redeposition. *Low accommodation siliciclastics* are associated with tidal-flat carbonates on the inner ramp. Although displaying high continuity in proximal areas, these rocks are typically mud-rich, poorly sorted and impermeable. *High accommodation siliciclastics* are associated with subtidal carbonates and were deposited in middle to outer ramp settings. These rocks are continuous in more distal platform areas but may display strike-elongate geometries.

Because their deposition is related to eustasy, siliciclastic deposits are potentially very valuable tools in sequence stratigraphic analysis. If accurately characterized, these rocks can provide more robust insights into the architecture of carbonate successions.

Geologic Setting

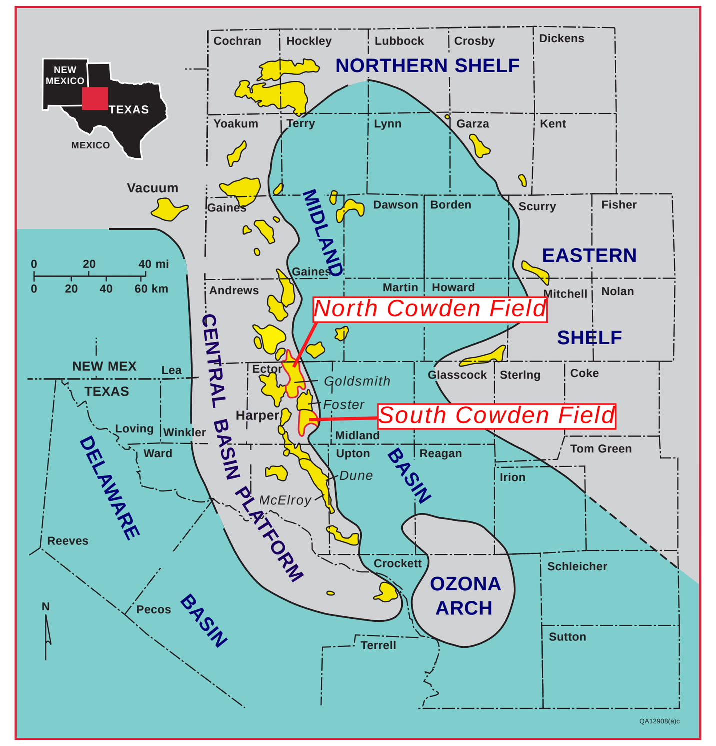

Paleogeographic map of the Permian Basin showing the locations of studied fields.

Sequence Stratigraphy

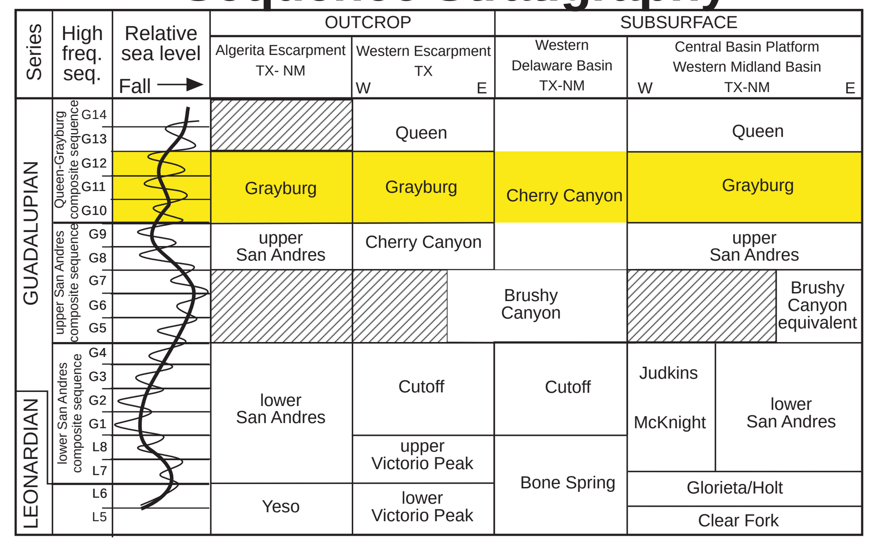

After Ruppel and Bebout (2001)

SETTING

Data

Cores (26 from South Cowden and 28 from North Cowden) were described to define facies and facies-stacking relationships. Core descriptions were integrated with wireline logs to develop sequence stratigraphic architecture.

South Cowden field
Paleogegraphy & Cored wells

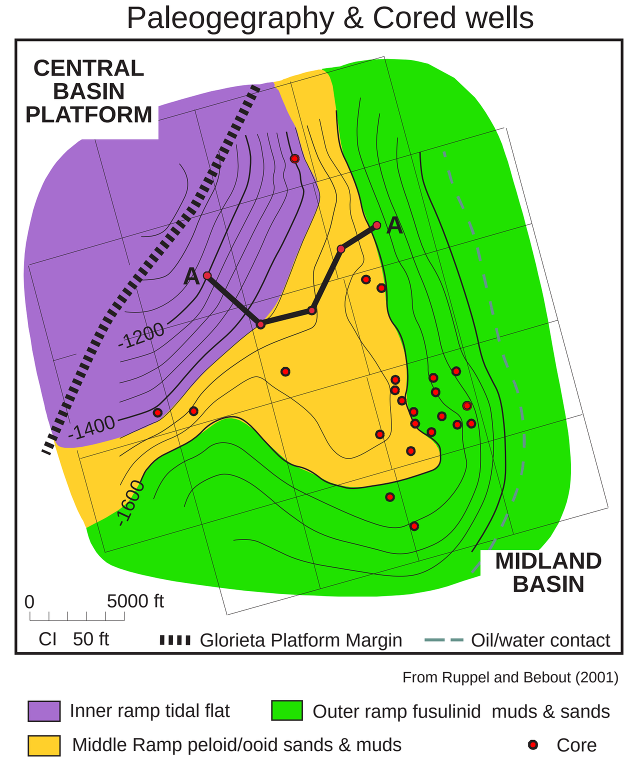

North Cowden field
Paleogeography & Cored wells

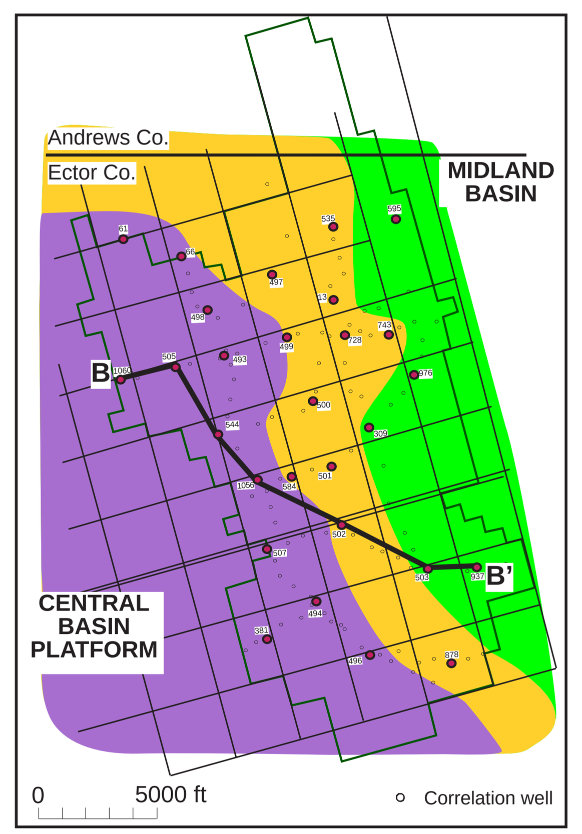

Grayburg carbonate depositional facies in the two field areas are very similar, as is the stratigraphic architecture. However, the reservoir successions differ markedly in the volume and distribution of siliciclastics despite being only 20 miles apart. This is related to North Cowden being farther north and thus closer to siliciclastic source areas in New Mexico and Colorado.

MIDDLE PERMIAN DEPOSITIONAL MODELS

Highstand Model

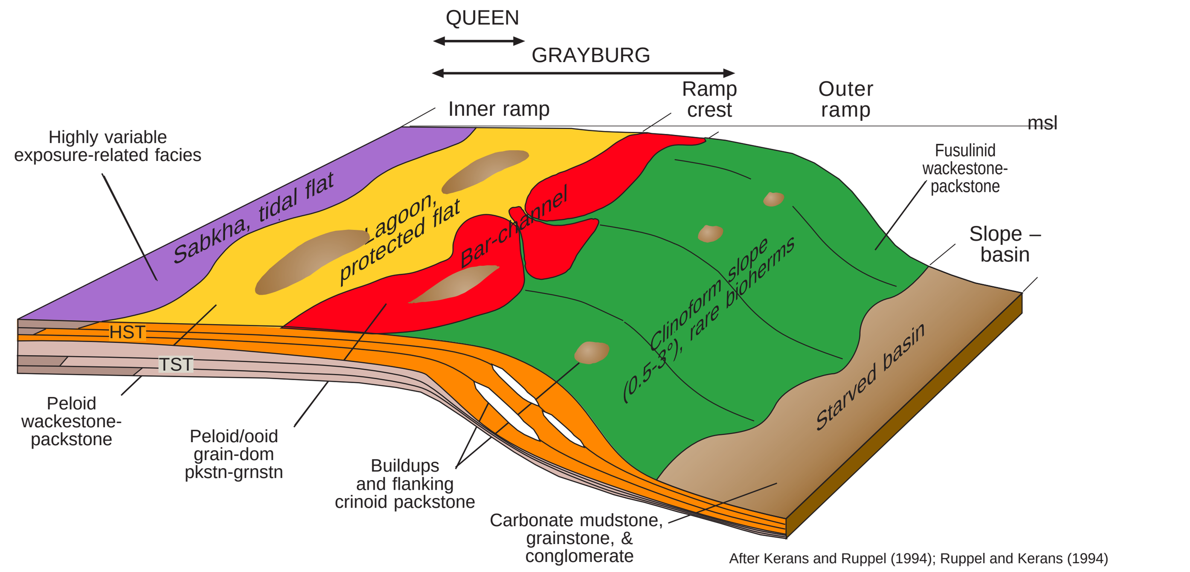

After Kerans and Ruppel (1994); Ruppel and Kerans (1994)

Carbonate facies and their dip-related spatial distributions on middle Permian platforms have been defined by C. Kerans and S. Ruppel based on outcrop and subsurface studies of Leonardian and Guadalupian successions across the Permian Basin. The above model depicts typical accommodation-controlled facies patterns during highstand.

Lowstand Model

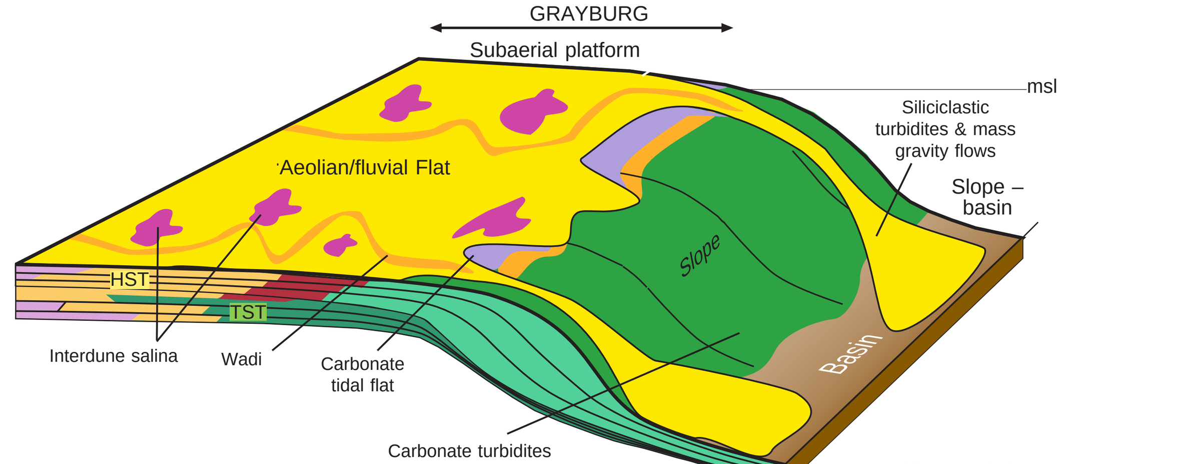

From Ruppel (in preparation)

Siliciclastics (fine-grained quartz sand, coarse-grained quartz silt, and clay) are transported onto Permian platforms during times of lower accommodation (e.g., late highstand, lowstand, and early transgression) when large areas are emergent. The above model depicts paleoenvironmental setting at lowstand. During lowstand, some siliciclastic sediments accumulate on the platform by aeolian and fluvial processes whereas others are transported off platform into the basins.

Sequence Model

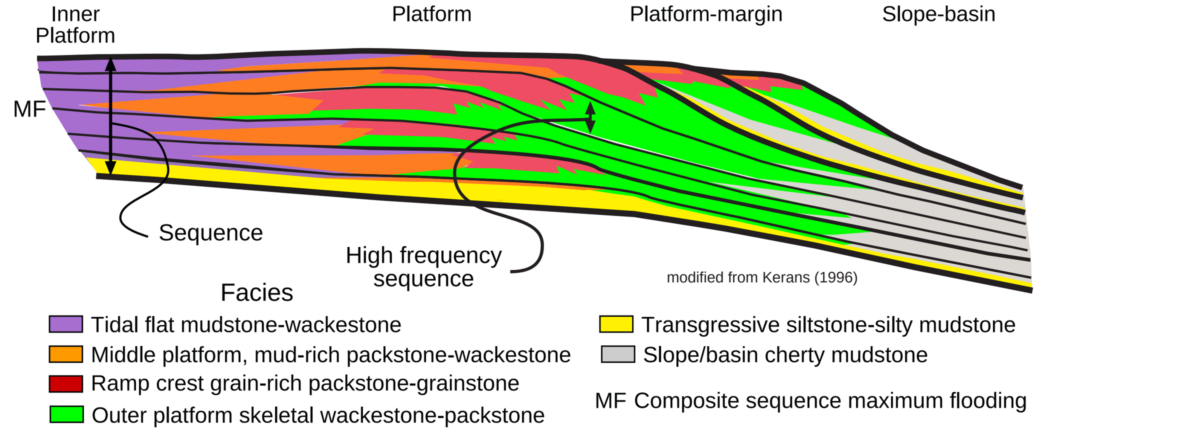

modified from Kerans (1996)

Facies
- Tidal flat mudstone-wackestone
- Middle platform, mud-rich packstone-wackestone
- Ramp crest grain-rich packstone-grainstone
- Outer platform skeletal wackestone-packstone
- Transgressive siltstone-silty mudstone
- Slope/basin cherty mudstone

MF Composite sequence maximum flooding

Siliciclastics abundance and distribution are a function of both eustasy and sediment supply. In areas of moderate siliciclastic sediment supply (as above and like South Cowden field) they may be restricted to sequence-scale late HST and LST systems tracts. However, where sediment supply is greater and/or accommodation is lower (like North Cowden) their distribution may be a function of cycle-scale eustasy.

DEPOSITIONAL FACIES

Carbonate-Dominated Facies

Tidal Flat Facies
- Ooid-peloidal-intraclast/pisolitic packstone-grainstone
- Pisolitic peloidal wackestone-packstone
- Algal-laminated mudstone-wackestone
- Massive mudstone

Subtidal Depositional Facies
- Peloidal wackestone
- Mollusk wackestone-mud-dominated packstone
- Burrowed, peloid wackestone-packstone
- Peloidal mud-dominated packstone
- Peloidal grain-dominated packstone
- Ooid grain-dominated packstone-grainstone
- Fusulinid wackestone-packstone

Siliciclastic-Dominated Facies
- Quartz sandstone-siltstone
- Quartzose mudstone-wackestone
- Cross-bedded quartz sandstone-siltstone

Carbonate-Dominated Facies

Carbonate Facies Model

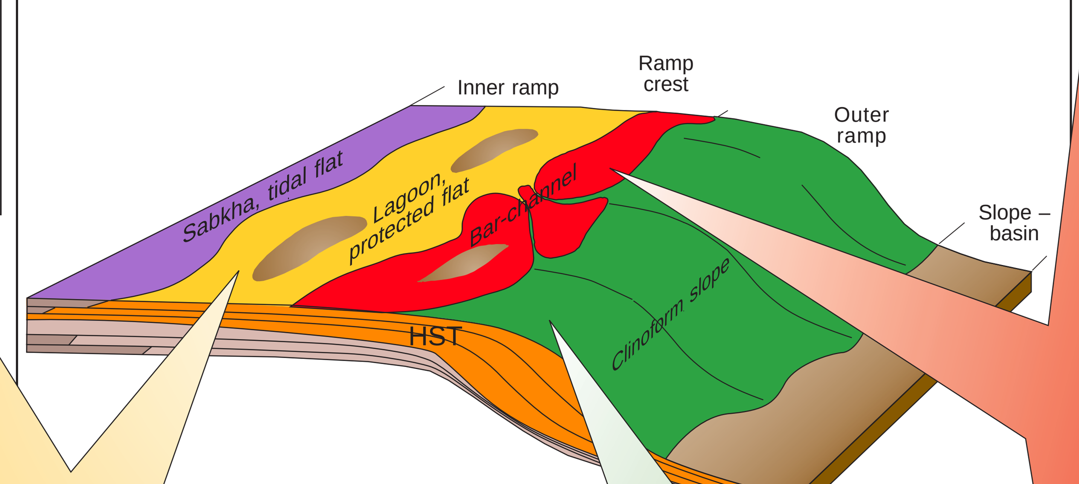

Inner Ramp Subtidal Facies

Peloidal Mud-Dominated Packstone
Cycle Top Facies

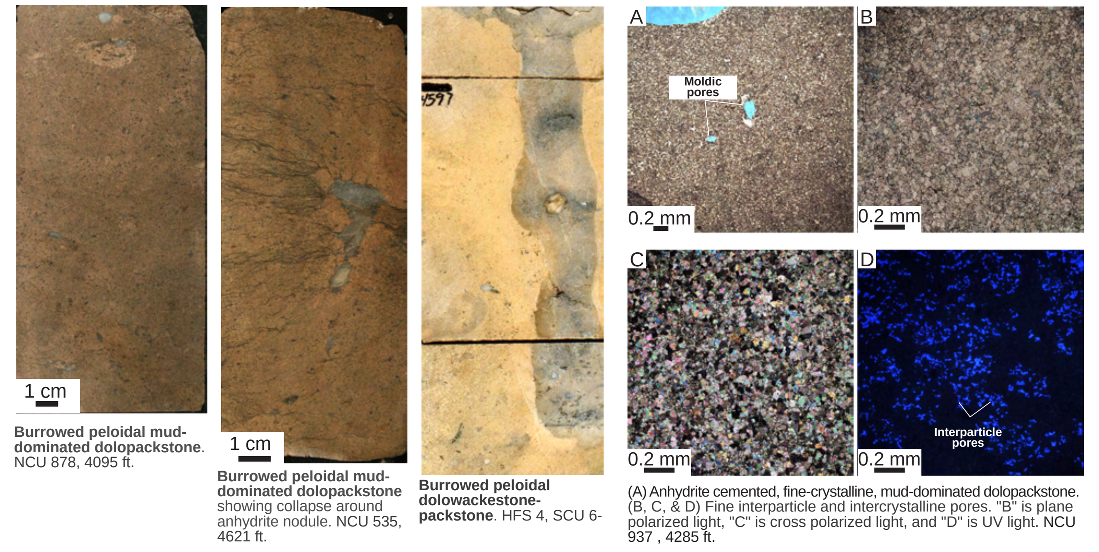

Mollusk Wackestone - Mud-Dominated Packstone
Cycle Base/Top Facies

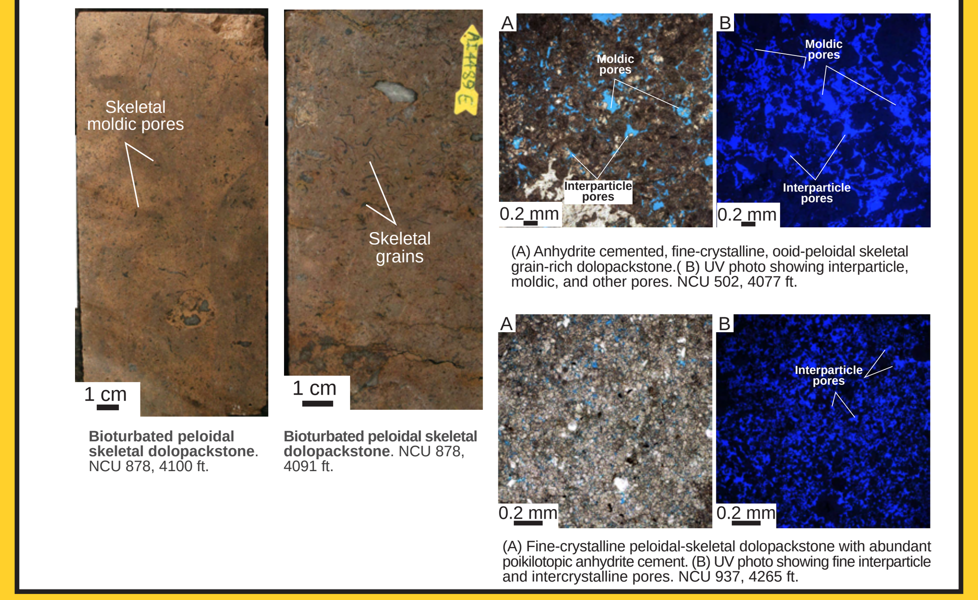

Peloidal Wackestone
Cycle Base Facies

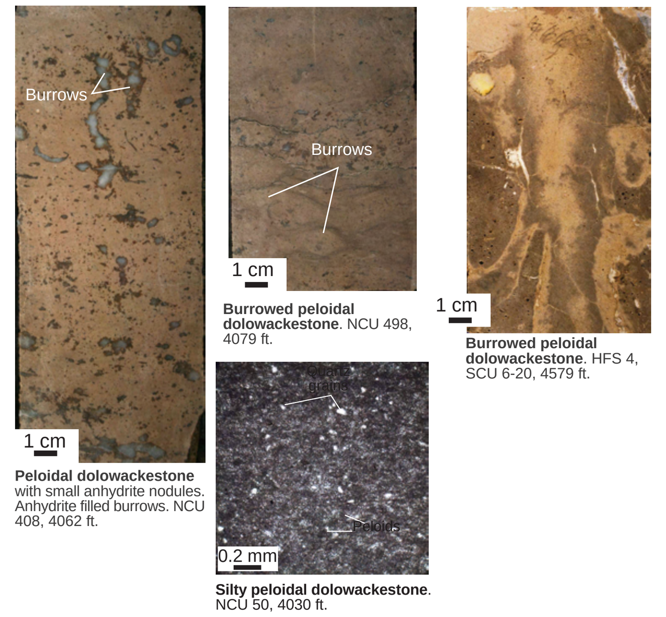

Ramp Crest Facies

Ooid Grain-Dominated Packstone to Grainstone
Cycle Top Facies

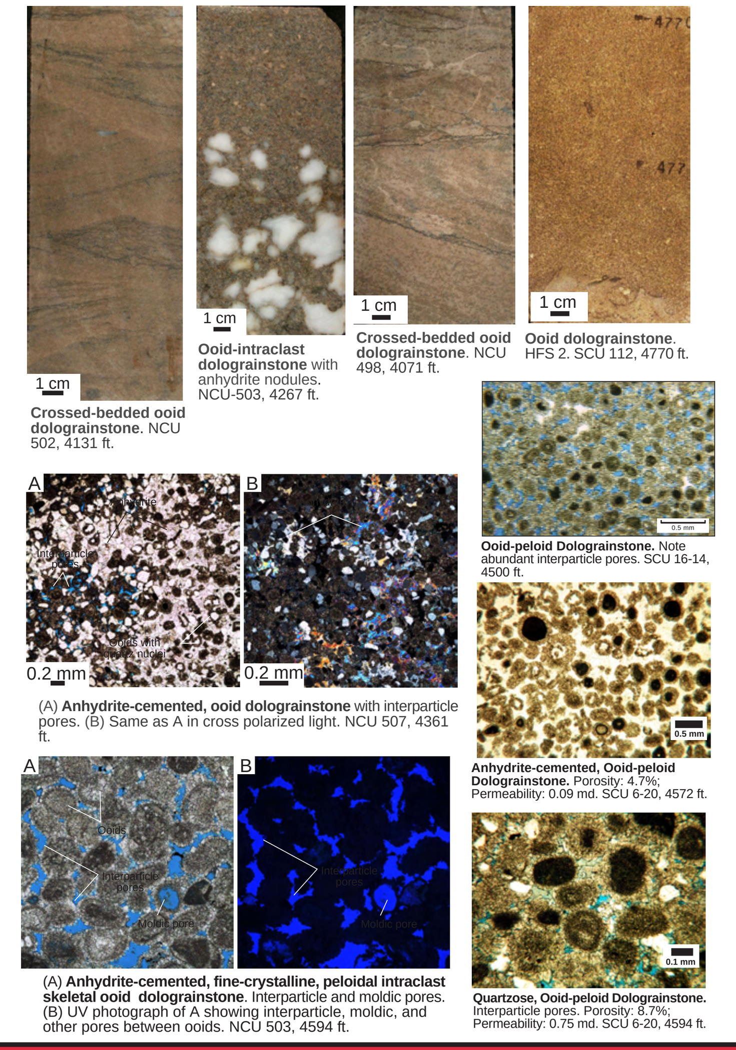

Peloidal Grain-Dominated Packstone
Cycle Top Facies

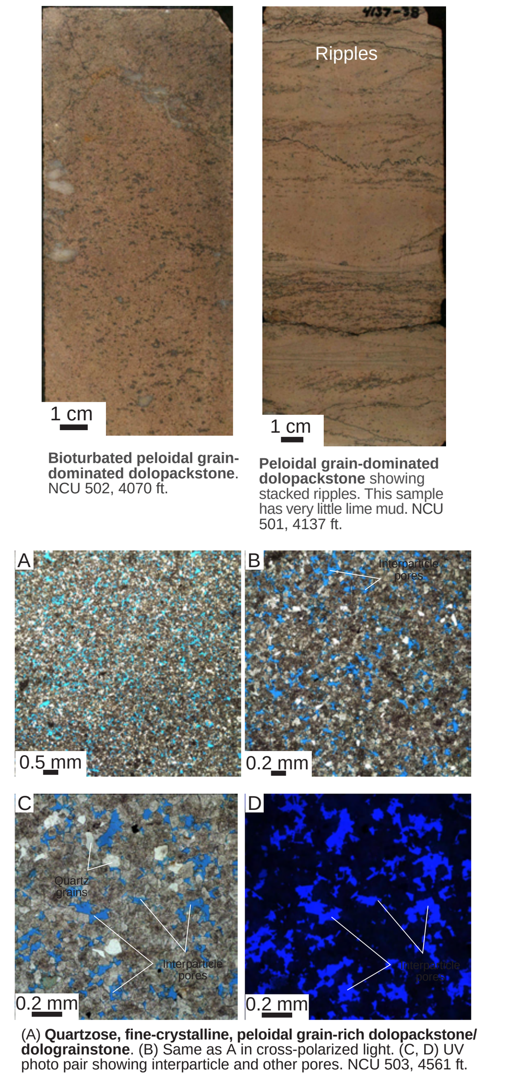

Outer Ramp Facies

Fusulinid Wackestone-Packstone
Cycle Base Facies

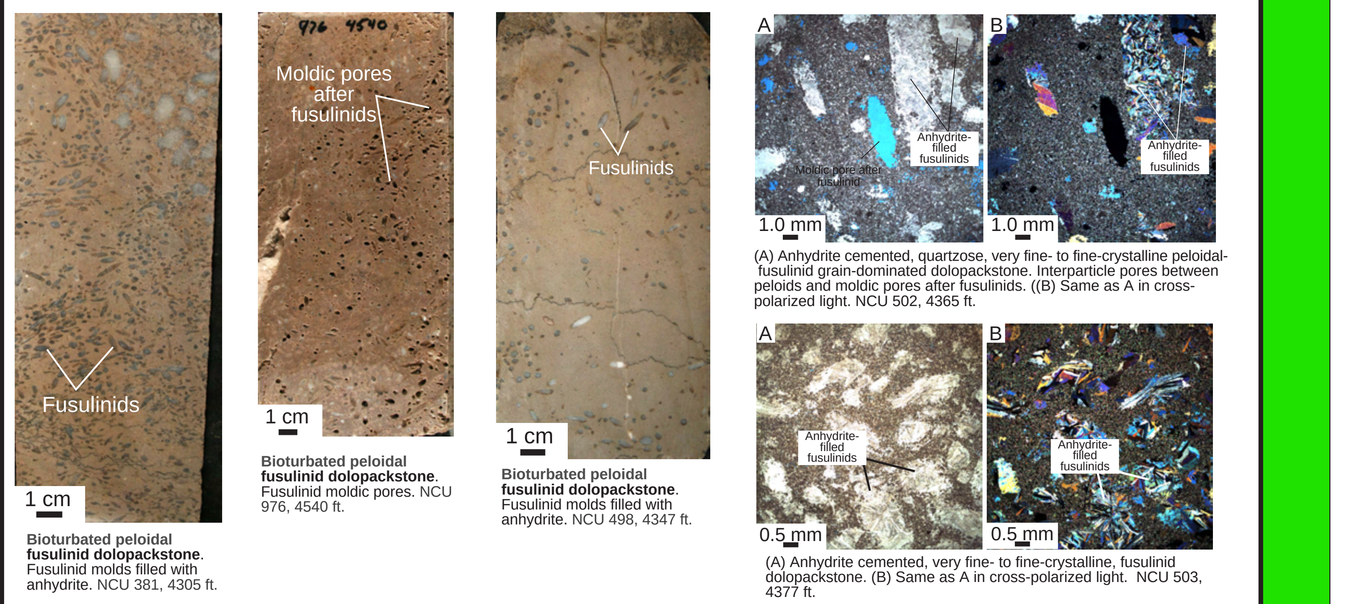

Bureau of Economic Geology

DEPOSITIONAL FACIES

DIAGENETIC FABRICS

Carbonate-Dominated Facies

Tidal-Flat Facies

Algal-Laminated Mudstone-Wackestone

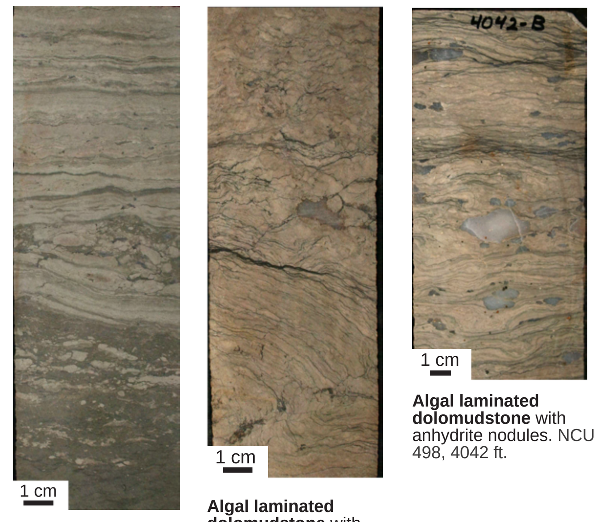

Algal laminated dolomudstone. Note disrupted algal mat in lower part of core - probably a storm erosion feature. NCU 61, 4462 ft.

Algal laminated dolomudstone with anhydrite nodules with contorted algal layers. NCU 61, 4136 ft.

Algal laminated dolomudstone with anhydrite nodules. NCU 498, 4042 ft.

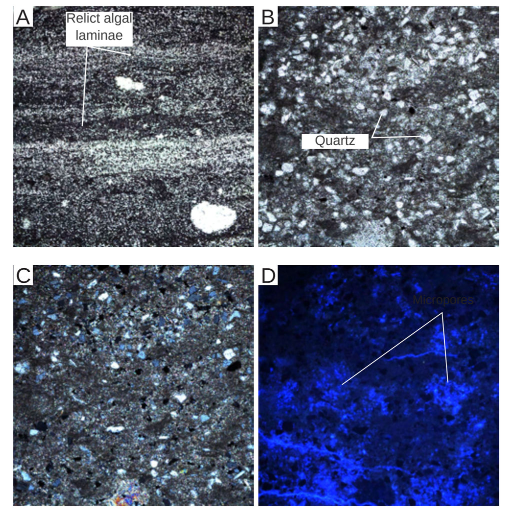

Algal laminated mudstone to wackestone. (A) Silty, algal dolowackestone (stromatolite). (B, C, & D) Photos showing details of stromatolite with micropores. B is plane-polarized light, C is cross-polarized light, and D is UV light. NCU 502, 4118 ft.

Pisolitic Peloidal Wackestone-Packstone

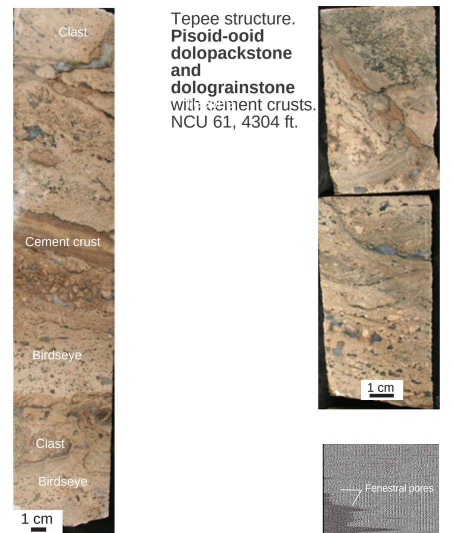

Tepee structure. Pisoid-ooid dolopackstone and dolograinstone with cement crusts. NCU 61, 4304 ft.

Pisolitic peloidal dolowackestone to dolopackstone with clasts and sheet cracks. Deposited on sabkha. NCU 728, 4335 ft.

Fenestral pisolitic peloidal dolopackstone. NCU 544, 3996.4 ft.

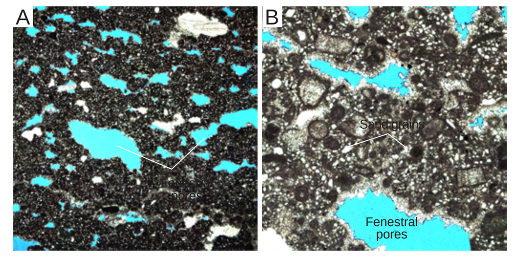

(A) Quartzose, peloidal-pisolitic, grain-rich dolopackstone with fenestral pores. (B) Close-up of A showing grains. NCU 503, 4587ft.

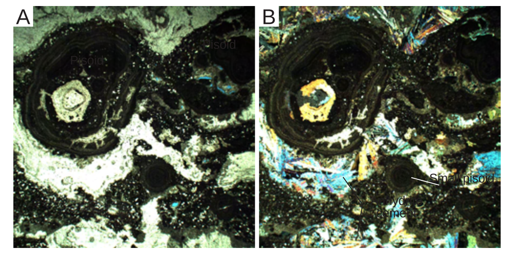

(A) Quartzose, very fine-crystalline, pisolitic-peloidal dolopackstone with anhydrite cement filling. Sample from a tepee structure. (B) Same as A in cross-polarized light. NCU 507, 3942

Ooid/peloidal/Intraclast Packstone-Grainstone

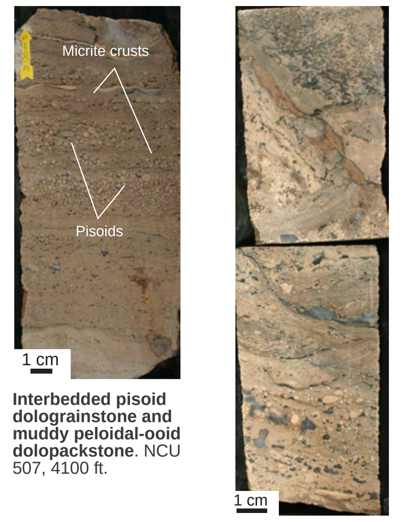

Interbedded pisoid dolograinstone and muddy peloidal-ooid dolopackstone. NCU 507, 4100 ft.

Tepee structure. Pisoid and ooid dolopackstone and dolograinstone. Note sheet cracks and cement crusts. NCU 61, 4304 ft.

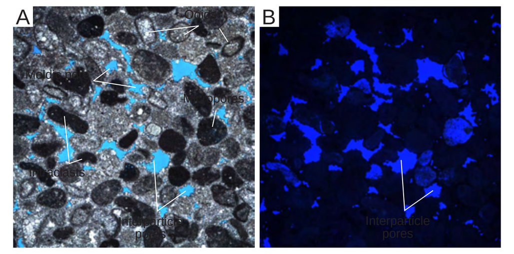

(A) Peloidal-intraclast-ooid dolograinstone with interparticle pores. Cemented by dolomite. (B) UV photograph of A showing interparticle, moldic, and micropores. NCU 502, 4411 ft.

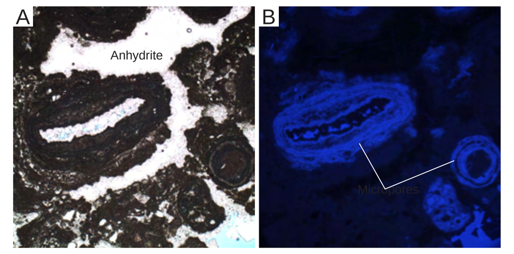

UV photo pair showing micropores in pisolite rims. NCU 507, 4126 ft.

Mudstone

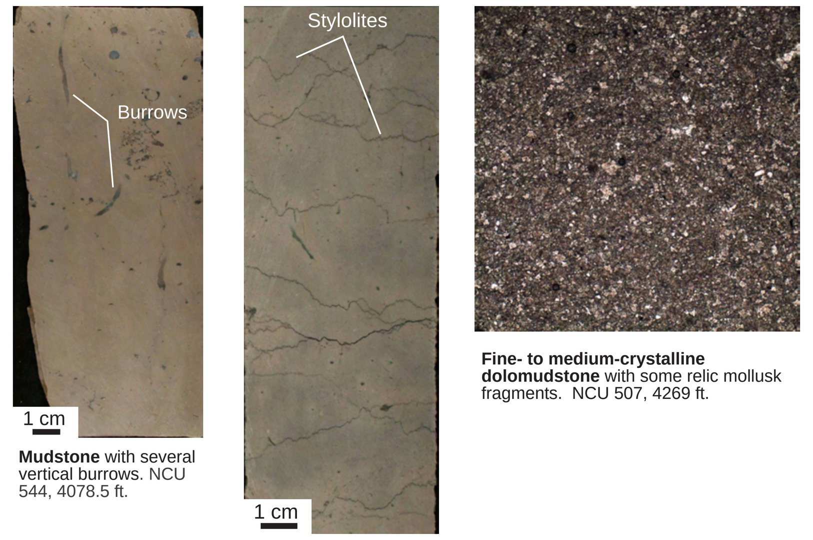

Mudstone with several vertical burrows. NCU 544, 4078.5 ft.

Mudstone with stylolites and faint oxidation/reduction alteration. NCU 61, 4130 ft.

Fine- to medium-crystalline dolomudstone with some relic mollusk fragments. NCU 507, 4269 ft.

Calcium Sulfate in Tidal Flats

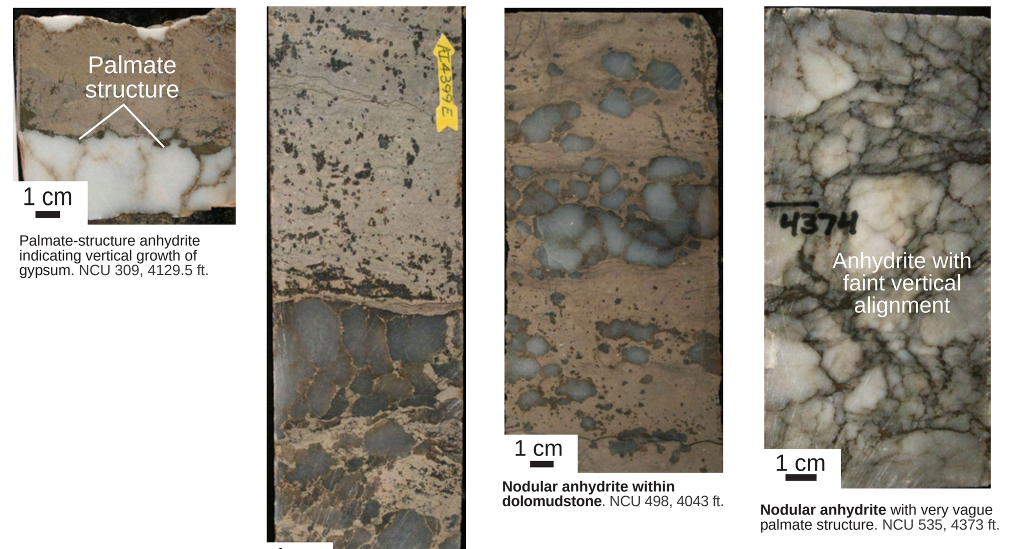

Palmate-structure anhydrite indicating vertical growth of gypsum. NCU 309, 4129.5 ft.

Nodular anhydrite within dolomudstone. NCU 498, 4043 ft.

Nodular anhydrite with very vague palmate structure. NCU 535, 4373 ft.

Palmate-structure anhydrite indicating vertical growth of gypsum. NCU 535, 4399 ft.

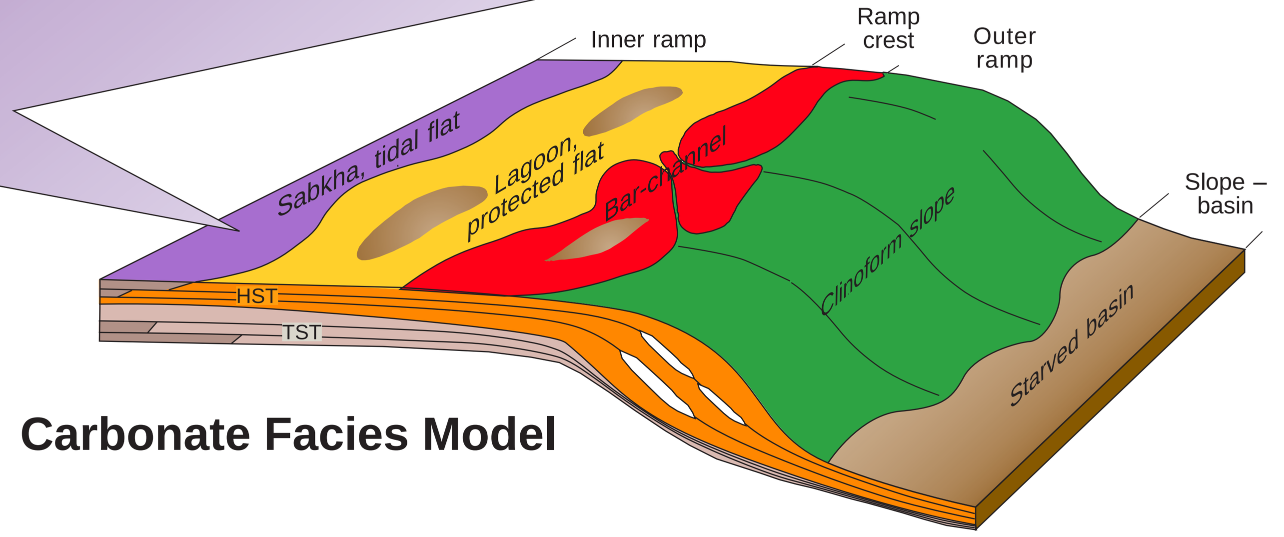

Carbonate Facies Model

Siliciclastic-Dominated Facies

Low Accommodation, Peritidal Siliciclastic Facies

Quartzose Mudstone-Wackestone

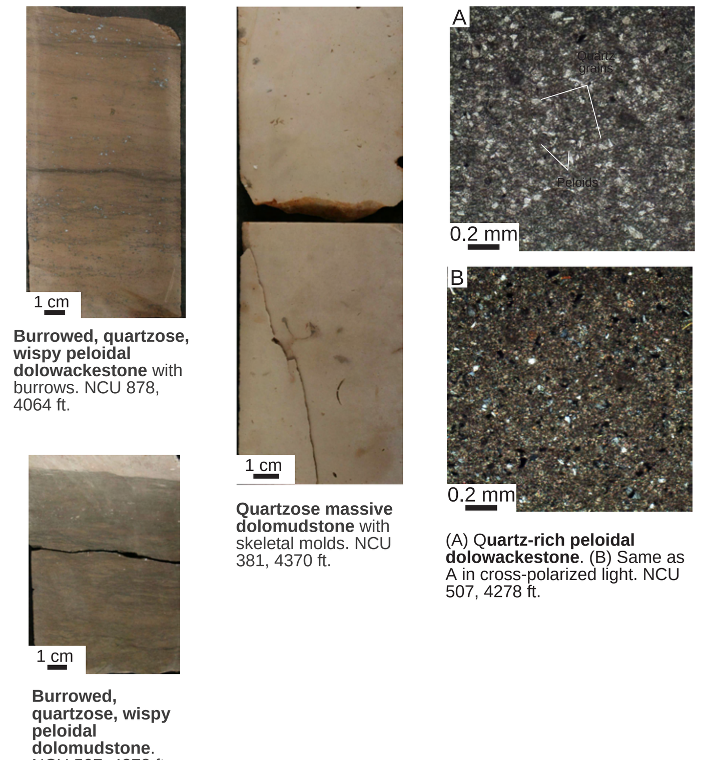

Burrowed, quartzose, wispy peloidal dolowackestone with burrows. NCU 878, 4064 ft.

Burrowed, quartzose, wispy peloidal dolomudstone. NCU 507, 4278 ft.

Quartzose massive dolomudstone with skeletal molds. NCU 381, 4370 ft.

(A) **Quartz-rich peloidal dolowackestone**. (B) Same as A in cross-polarized light. NCU 507, 4278 ft.

Quartz Sandstone-Siltstone

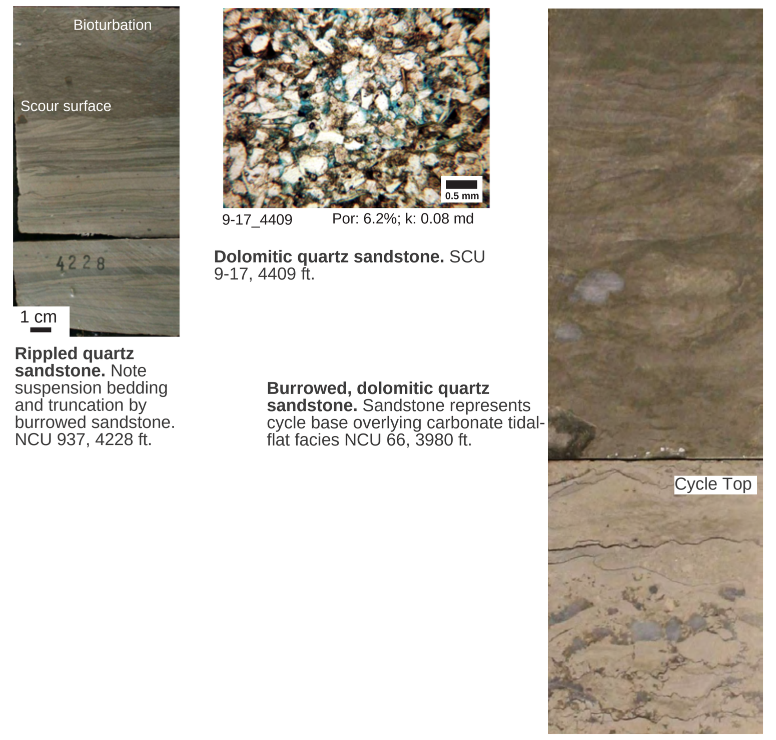

Rippled quartz sandstone. Note suspension bedding and truncation by burrowed sandstone. NCU 937, 4228 ft.

Dolomitic quartz sandstone. SCU 9-17, 4409 ft.

Burrowed, dolomitic quartz sandstone. Sandstone represents cycle base overlying carbonate tidal-flat facies NCU 66, 3980 ft.

Higher Accommodation, Subtidal Siliciclastic Facies

Cross-bedded Sandstone-Siltstone

Cross-bedded quartz sandstone. NCU 496, 4254 ft.

Rippled quartz sandstone. Abundant anhydrite cement. NCU 535, 4355 ft.

Cross-bedded quartz sandstone with abundant anhydrite cement. NCU 381, 4267 ft.

Massive anhydrite-cemented quartz sandstone. NCU 502, 4244 ft.

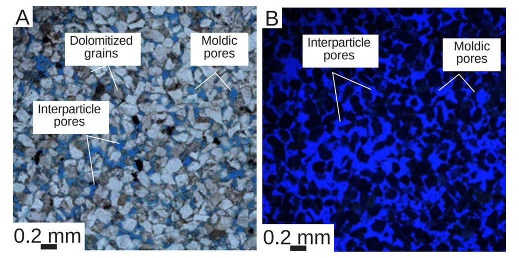

Quartz siltstone and sandstone (subarkose): (A) Very fine- to fine-grained subarkose with anhydrite cement. Note abundant interparticle pores and minor moldic pores. Cross-polarized light. (B) Same as A in UV light. NCU 502, 4247 ft.

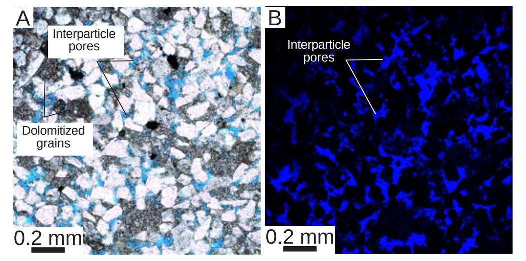

Quartz siltstone and sandstone (subarkose): (A) Very fine- to fine-grained subarkose with dolomitic peloids and minor anhydrite cement. Pore network of interparticle pores. (B) Same as A in UV light. Note pores. NCU 502, 4241 ft.

Karst/Dissolution Fabrics

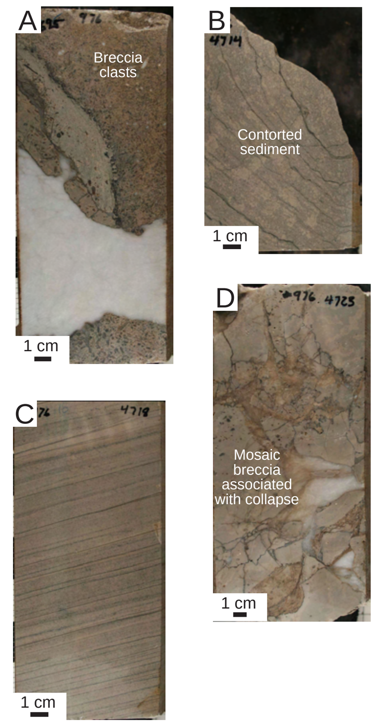

Karst Breccias: (A) Breccias at top of large vug. NCU 976, 4695 ft. (B) Distorted sediment within vug may indicate the brecciation occurred while sediment was firm and not totally lithified. This would indicate near-surface dissolution and collapse. NCU 976, 4714 ft. (C) Laminated quartz-sand fill within vugs, suggesting that dissolution was early and shallow. NCU 976, 4718 ft. (D) Mosaic breccias near base of the large vug. Interclast pores filled with anhydrite cement. NCU 976, 4723 ft.

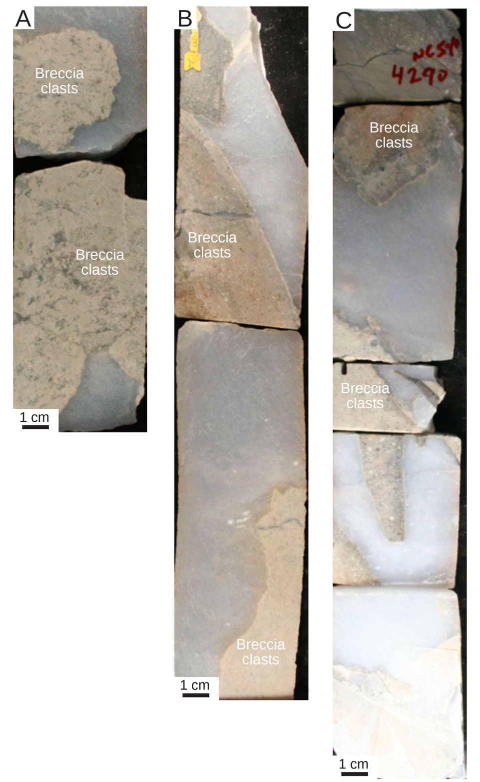

Karst Breccias: (A-C) Breccia clasts with interclast anhydrite cement. NCU 544, 4286 - 4290 ft.

Anhydrite Dissolution Fabrics

Sulfate Diagensis

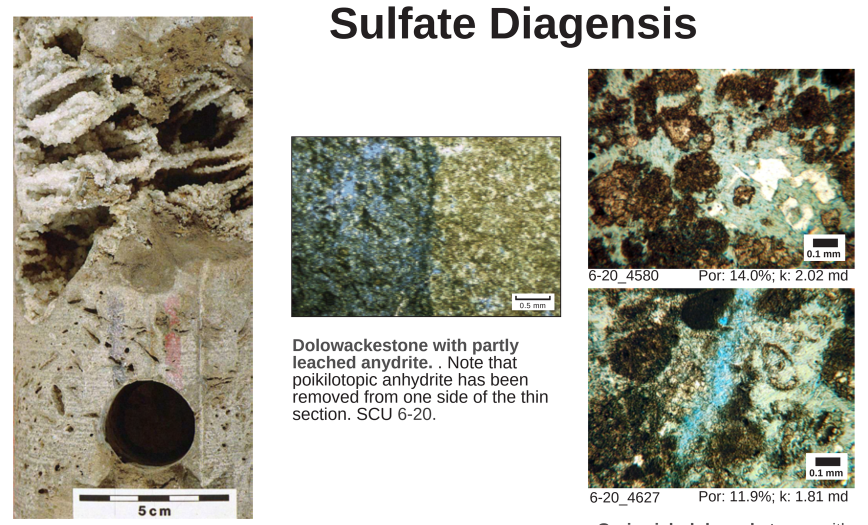

Peloidal fusulinid dolopackstone. Note that anhydrite has been removed from both nodules and fusulinid molds by late stage dissolution. SCU 6-20, xxxx ft.

Dolowackestone with partly leached anydrite. . Note that poikilotopic anhydrite has been removed from one side of the thin section. SCU 6-20.

Grain-rich dolopackstones with areas of altered (bassanite) and leached anydrite. SCU.

Burrow-related Dolomite Diagenesis

Burrowed peloidal fusulinid dolopackstone. Alteration of dolomite around burrows has resulted in a twofold increase in porosity and an order of magnitude increase in permeability. SCU 6.20.

Bureau of Economic Geology

DEPOSITIONAL ARCHITECTURE

Cyclicity

High-frequency cycles (or repeated facies successions) are observed in cores in both field areas. Cycles commonly range from 10 - 15 ft in thickness but are most readily defined where facies contrasts are greatest. At South Cowden field, this is largely limited to ramp crest areas. Correlations of carbonate facies and cycles are problematic, however.

Inner Ramp Facies-Stacking Patterns

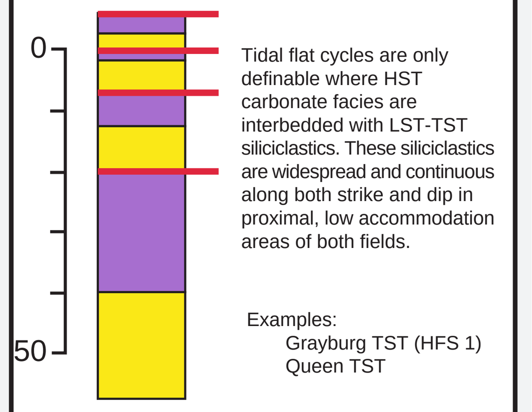

Tidal flat cycles are only definable where HST carbonate facies are interbedded with LST-TST siliciclastics. These siliciclastics are widespread and continuous along both strike and dip in proximal, low accommodation areas of both fields.

Examples: Grayburg TST (HFS 1) Queen TST

Ramp Crest Facies-Stacking Patterns

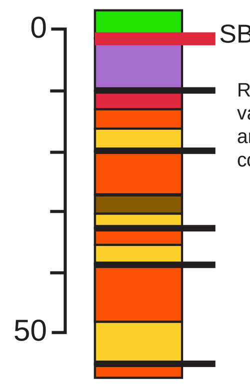

Ramp crest stacking patterns vary laterally due to facies amalgamation and are not correlative at the cycle scale.

Outer Ramp Facies-Stacking Patterns

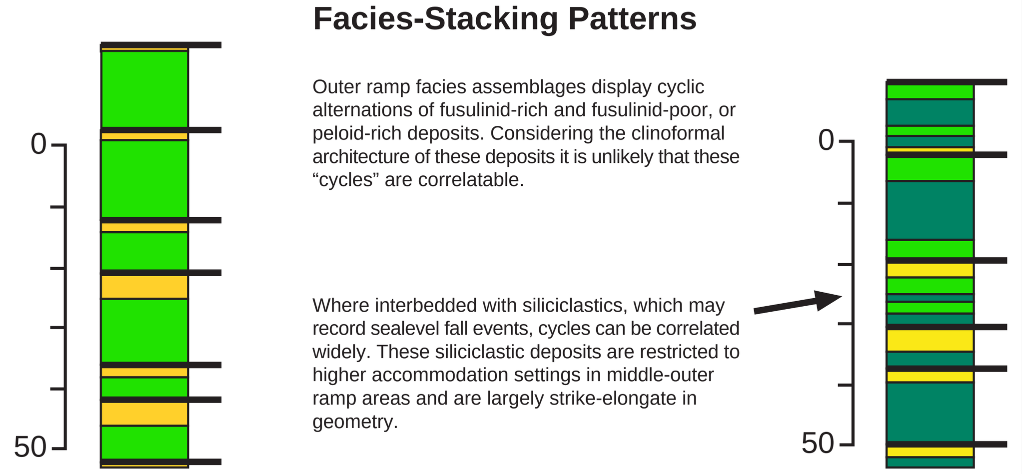

Outer ramp facies assemblages display cyclic alternations of fusulinid-rich and fusulinid-poor, or peloid-rich deposits. Considering the clinoformal architecture of these deposits it is unlikely that these "cycles" are correlatable.

Where interbedded with siliciclastics, which may record sealevel fall events, cycles can be correlated widely. These siliciclastic deposits are restricted to higher accommodation settings in middle-outer ramp areas and are largely strike-elongate in geometry.

Wireline-Log Definition of Cycles

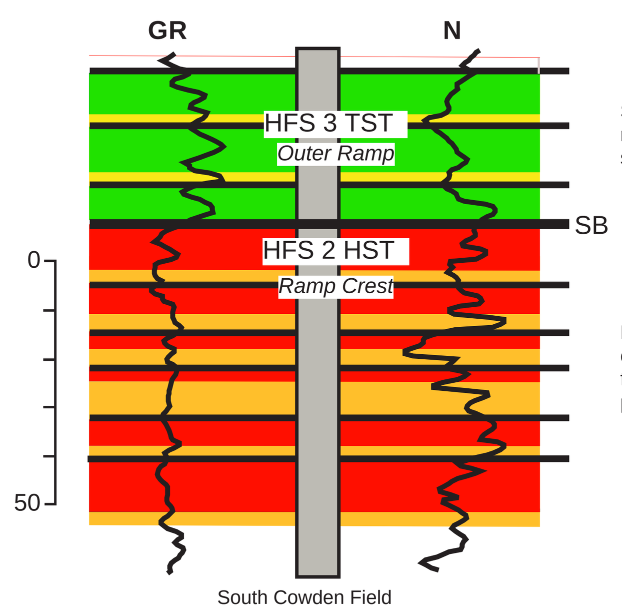

Siliciclastic beds are defined in many log suites making cycle scale correlations of these cycle scale events feasible.

Because of diagenesis, log response to carbonate facies changes is variable. Thus, fieldwide correlations at the cycle scale are not possible.

Facies
- Tidal Flat
- Sandstone-sandstone
- Peloid wackestone-packstone
- Peloid/ooid packestone-grainstone
- Ooid grainstone
- Fusulinid wackestone-packstone
- Peloid-fusulinid-packstone

Cycle/Sequence Boundaries
- HFS
- Cycle

Sequence Stratigraphy

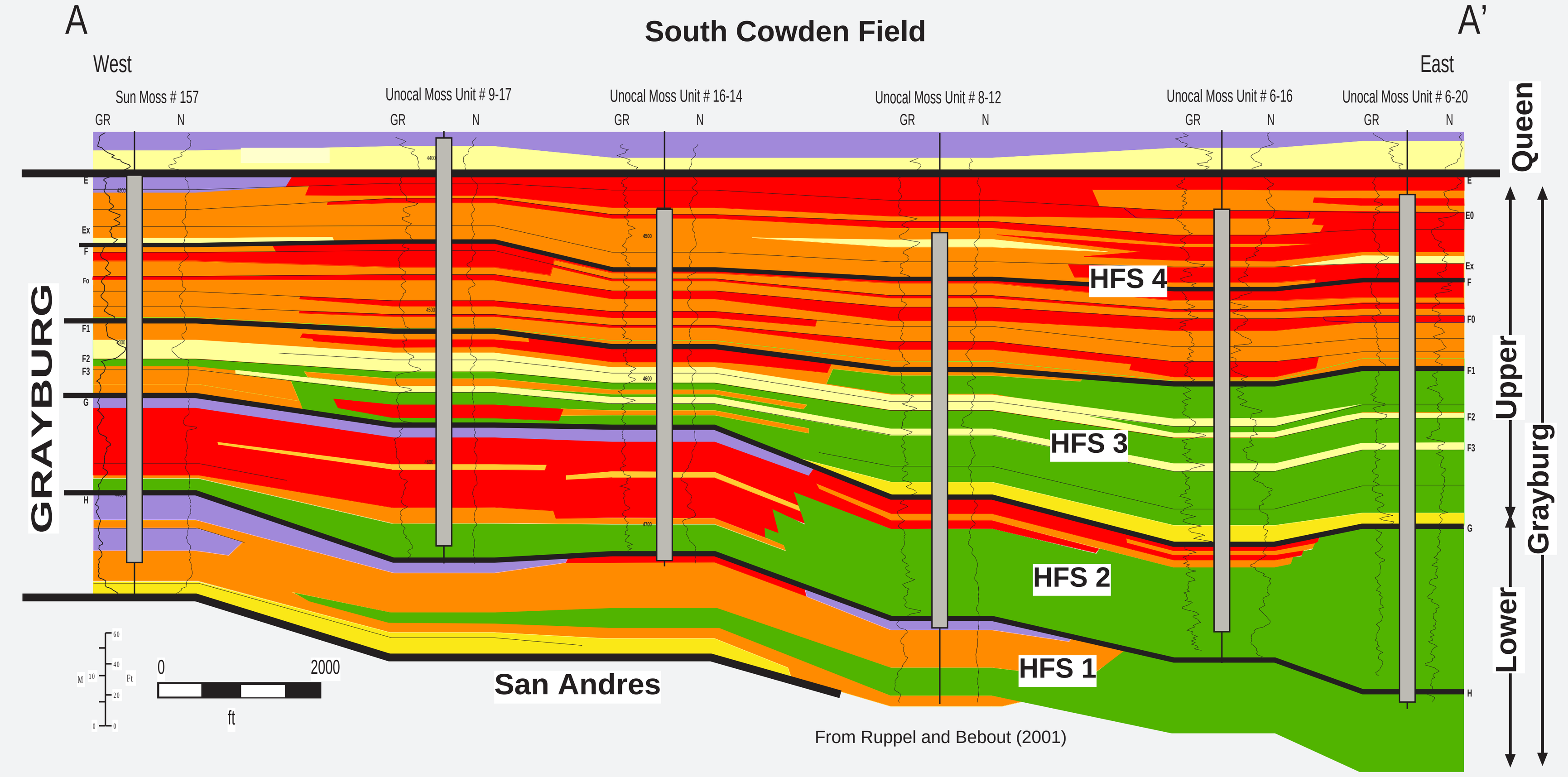

From Ruppel and Bebout (2001)

Core-based facies studies *do* provide robust insights into the sequence-scale architecture of the Grayburg at both fields. At South Cowden, carbonate facies were used to define an accommodation-based sequence stratigraphy comprising four high-frequency sequences. Siliciclastic deposits are restricted to HFS 3 and the overlying Queen Fm.

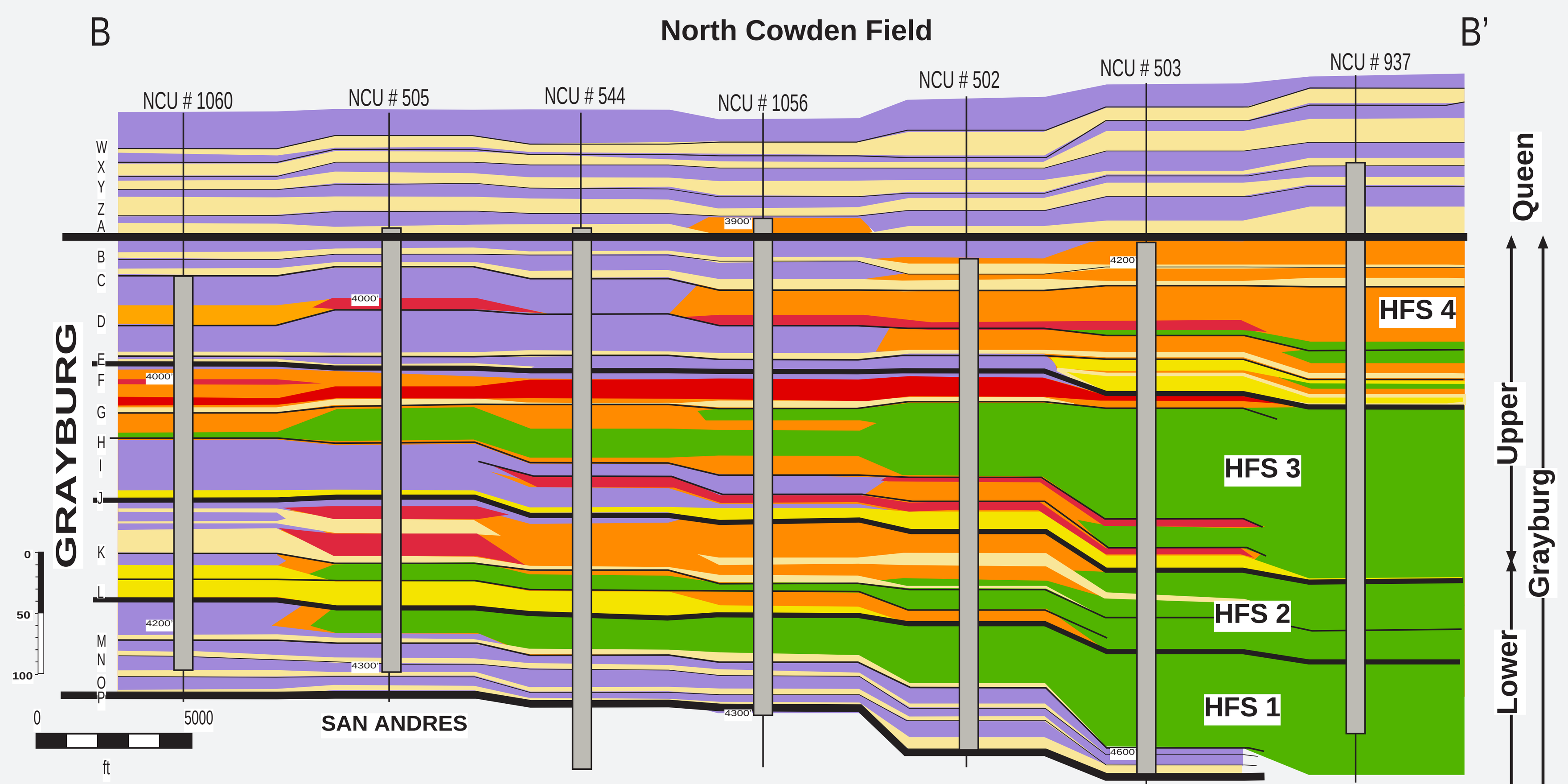

Unlike South Cowden, the Grayburg at North Cowden contains abundant siliciclastic deposits. The distribution of these deposits provides key information on sequence architecture, some of which seems inconsistent with the accommodation story suggested by carbonate facies patterns alone. The abundance of the siliciclastics is a function of many factors. Their geometries, however, are a function of accommodation.

Facies Tracts
- Tidal Flat
- Low accommodation siltstone-sandstone
- High accommodation siltstone-sandstone
- Inner - Middle ramp peloid/ooid wackestone-grainstone
- Ramp Crest peloid/ooid grainstone
- Outer Ramp fusulinid wackestone-packstone
- G Marker bed
- Cored interval

Cycle/Sequence Boundaries
- Composite Sequence top
- HFS top
- Cycle/Cycle Set top

GEOMETRIES AND DISTRIBUTION OF SILICICLASTICS

High Accommodation, Distal Siliciclastics

These siliciclastic deposits accumulate on the middle to outer shelf during LST and the ensuing TST. They are typically strike-elongate, their updip limits controlled by more proximal, ramp crest and/or tidal flat topography. They are thickest near this updip terminus and thin downdip. Because of their higher accommodation setting, they are typically better sorted.

North Cowden field

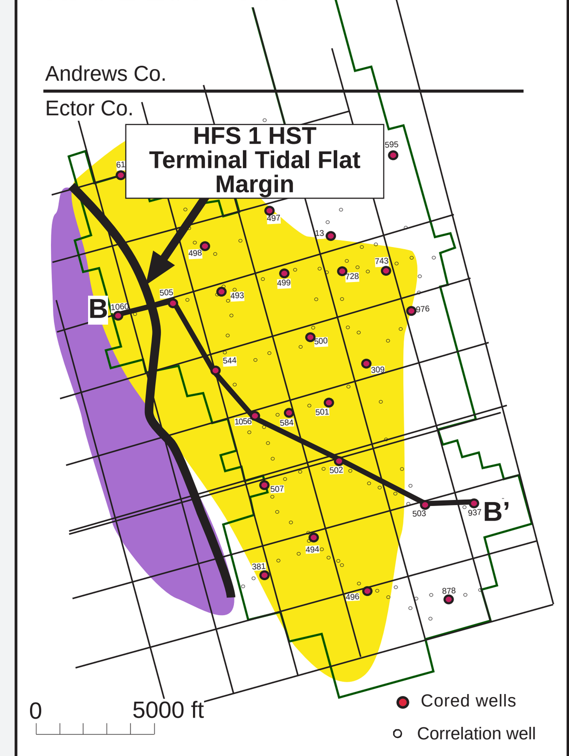

HFS 1 HST
- Tidal flat

HFS 2 LST-TST
- High accommodation siliciclastics

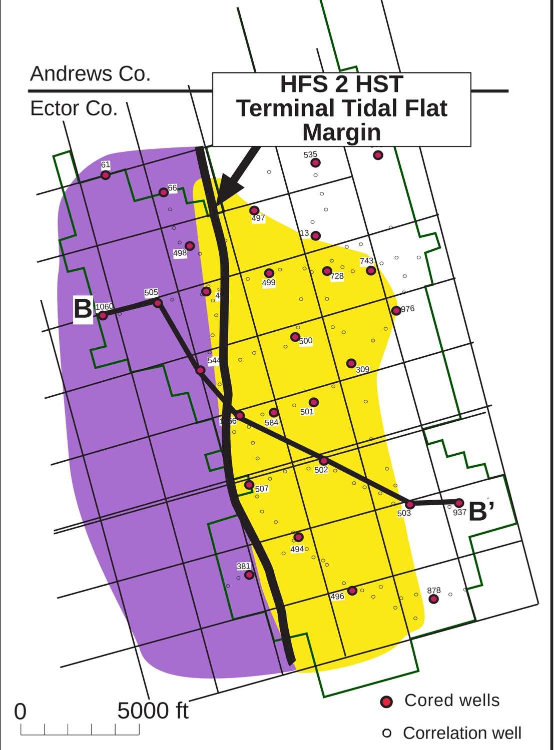

HFS 2 HST
- Tidal flat

HFS 3 LST-TST
- High accommodation siliciclastics

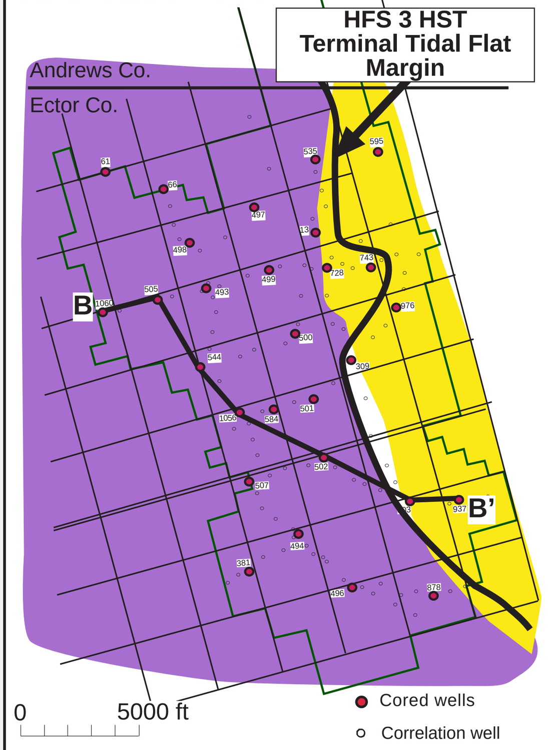

HFS 3 HST
- Tidal flat

HFS 4 LST-TST
- High accommodation siliciclastics

South Cowden field

Grayburg HFS 3 LST - TST

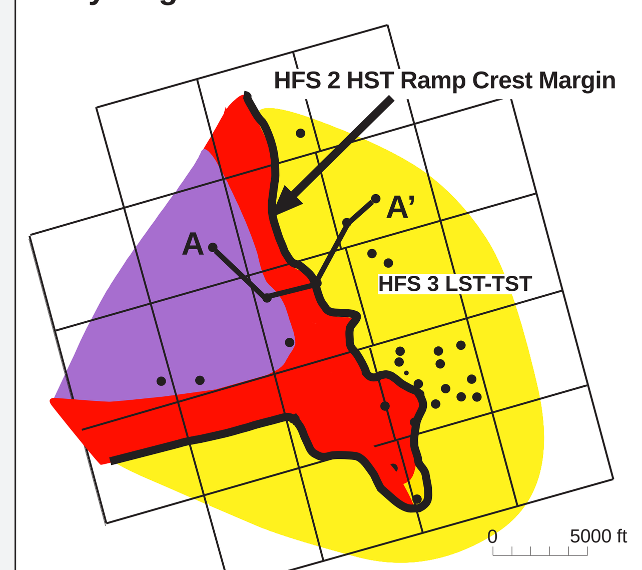

HFS 2 HST
- Peloid-ooid grainstone
- Tidal flat

HFS 3 LST-TST
- High accommodatio siliciclastics

• Cored wells

Grayburg HFS 3 HST

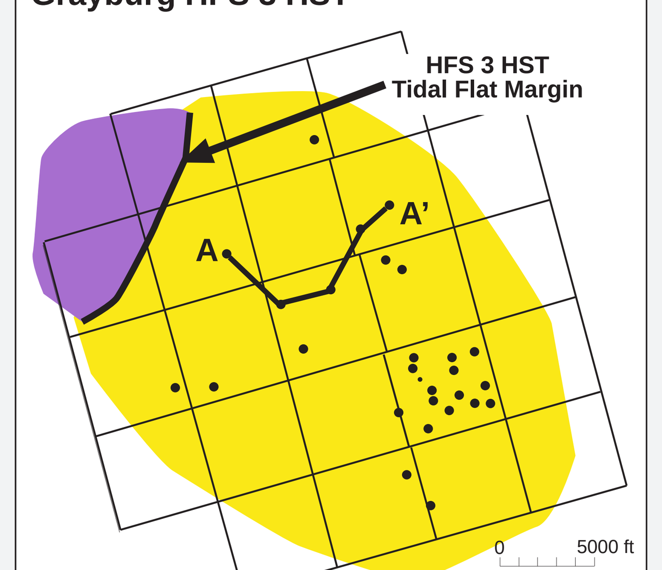

HFS 3 HST
- Tidal flat

HFS 3 TST- HST
- High accommodation siliciclastics

• Cored wells

The siliciclastic deposits at the base of HFS 3 at South Cowden are virtually identical to those at North Cowden. The deposits in the overlying section may reflect a period of increased sediment input.

Low Accommodation, Proximal Siliciclastics

Low accommodation siliciclastics accumulated on the inner ramp and are invariably associated with tidal-flat carbonates. Because of the generally flat-lying topography, they are highly continuous over large areas. These rocks are typically more poorly sorted and clay-rich due the low-energy setting..

North Cowden field

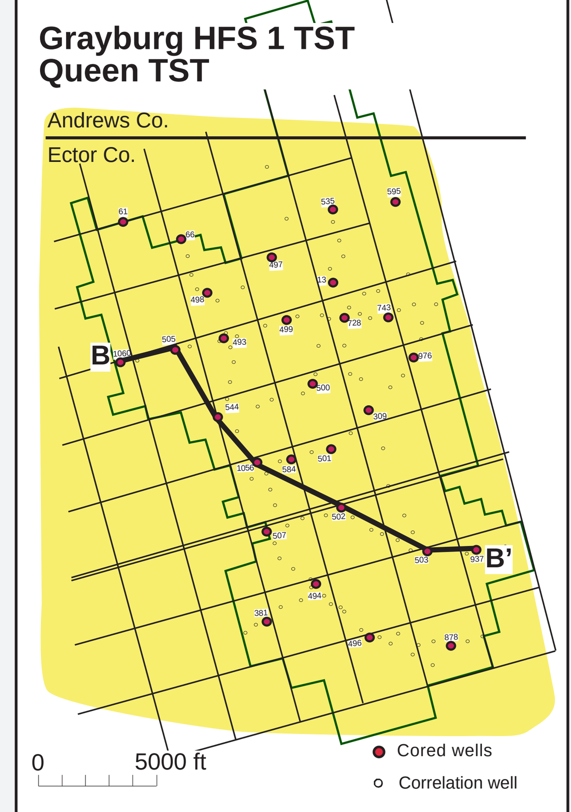

- Low accommodation siliciclastics

South Cowden field

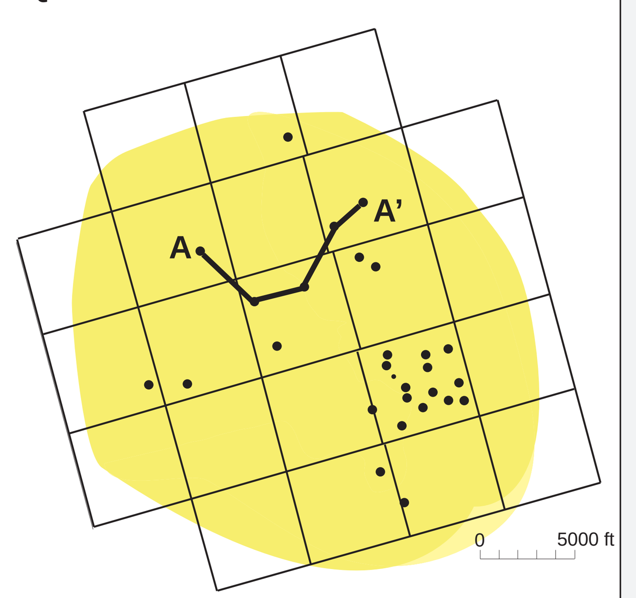

- Low accommodation siliciclastics
- • Cored wells

Integrated Sequence Model of Siliciclastic and Carbonate Geometries

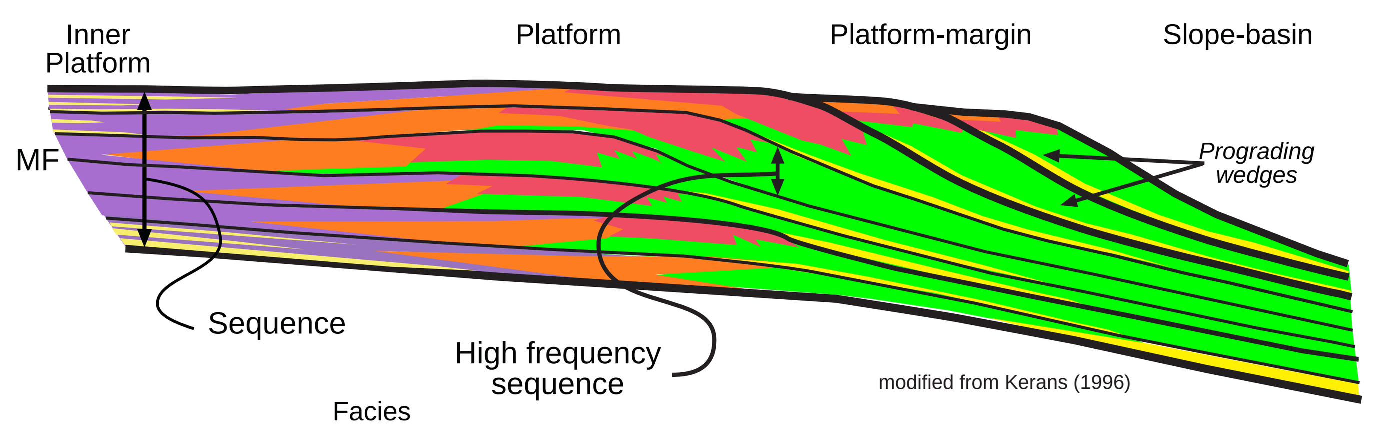

modified from Kerans (1996)

Facies
- Tidal flat mudstone-wackestone
- Middle platform, mud-rich packstone-wackestone
- Ramp crest grain-rich packstone-grainstone
- Outer platform skeletal wackestone-packstone
- High accommodation, distal siliciclastics
- Low accommodation, proximal siliciclastics

MF Composite sequence maximum flooding

Siliciclastic deposits are most abundant at cycle and sequence bases reflecting (1) their transport across the platform during sealevel lowstand and subsequent reworking during sealevel rise and (2) decreased supply during maximum flooding. Importantly, inner platform and middle/outer platform deposits are not linked and vary in geometries and facies.

CONCLUSIONS

1. Siliciclastic deposits in carbonate successions can exhibit wide variations in abundance, distribution, geometry (e.g., thickness, extent), facies, and reservoir quality.

2. Many of these differences are tied to variations in depositional accommodation across the platform.

3. *Low accommodation siliciclastics* accumulated in low-energy, inner-ramp settings and are associated with tidal-flat carbonates. Although of high continuity, they are commonly mud-rich and exhibit poor reservoir quality.

4. *High accommodation siliciclastics* are associated with higher energy middle and outer ramp carbonates. These deposits form distal, strike-elongate trends of well sorted, high-porosity and permeability reservoir rocks.

5. Although overall siliciclastic sediment flux is a function of many drivers (e.g., climate, tectonics, eustasy), both types of siliciclastic deposits appear to be related to sealevel rise (i.e., transgressive) events.

6. As such, they form excellent tools for defining sequence-scale and high-frequency sequence-scale boundaries.

7. It important to note that these two types of deposits are not laterally equivalent or correlative. Thus, distinguishing the two has important significance for modeling reservoir architecture and productivity.

ACKNOWLEDGEMENTS

We thank OXY Permian for access to data from North Cowden (NC) field and the right to publish our findings. Special thanks to Thorbjorn Peterson and Sam Scott for their insights about the geology at NC. Don Bebout, Jerry Lucia, and Charlie Kerans contributed to our ideas about facies and reservoir architecture at South Cowden (DB, JL, CK) and NC (CK) reservoirs.

PUBLICATIONS

South Cowden Field

Ruppel, S. C., Park, Y. J., and Lucia, F. J., 2002, Applications of 3-D seismic to exploration and development of carbonate reservoirs: South Cowden Grayburg field, West Texas, in Hunt, T. J., and Lufholm, P. H., eds., The Permian Basin: preserving our past—securing our future: West Texas Geological Society, Publication No. 02-111, p. 71–87.

Ruppel, S. C., and Bebout, D. G., 2001, Competing effects of depositional architecture and diagenesis on carbonate reservoir development: Grayburg Formation, South Cowden field, West Texas: The University of Texas at Austin, Bureau of Economic Geology Report of Investigations No. 263, 62 p.

Lucia, F. J., 2000, Petrophysical characterization and distribution of remaining mobile oil: South Cowden Grayburg reservoir, Ector County, Texas: The University of Texas at Austin, Bureau of Economic Geology Report of Investigations No. 260, 54 p.

Jennings, J. W., Jr., Lucia, F. J., and Ruppel, S. C., 1998, Waterflood performance modeling for the South Cowden Grayburg reservoir, Ector County, Texas: The University of Texas at Austin, Bureau of Economic Geology Report of Investigations No. 247, 46 p.

Lucia, F. J., and Ruppel, S. C., 1996, Characterization of diagenetically altered carbonate reservoirs, South Cowden Grayburg reservoir, West Texas: Society of Petroleum Engineers, Paper SPE 36650, p. 883–893.

Ruppel, S. C., and Lucia, F. J., 1996, South Cowden Grayburg field, Ector County, Texas, in Oil and gas fields in West Texas, volume VII: West Texas Geological Society, Publication No. 96-99, p. 39–48.